This is a post-peer-review, pre-copyedit version of an article published in **IECON 2014 - 40th Annual Conference of the IEEE Industrial Electronics Society**. The final authenticated version is available online at: https://doi.org/10.1109/IECON.2014.7048888

Analytical Modelling of the Multicell Piezoelectric Motor Based on Three Resonance Actuators

R. Ryndzionek, M. Michna, , M. Ronkowski
Faculty of Electrical and Control Engineering
Gdansk University of Technology
Gdansk, Poland
ryndzionek@ely.pg.gda.pl, michna@pg.gda.pl

J-F. Rouchon
Laboratoire Plasma et Conversion d'Energie (LAPLACE),
ENSEEIHT – INPT,
Toulouse, France
rouchon@laplace.univ-tlse.fr

***Abstract*— Abstract— This paper presents analytical model of the multicell piezoelectric motor. The results, obtained in the field of piezoelectric motors, have pointed out that these motors have potentially high possibilities in the future of special applications. The studied multicell piezoelectric motor have a stator using three rotating mode actuators. A theoretical analysis of operating principle of the rotating mode motor has been described. Additionally the stator/rotor friction contact has been considered. Using the analytical model some electromechanical characteristics of the considered multicell piezoelectric motor have been computed. Finally, computed and measured characteristics have been compared.**

Keywords*— *piezoelectricity, piezoelectric actuator, piezoelectric motor, rotating-mode motor, traveling wave motor

I. INTRODUCTION

Most of the mechatronic drive systems use electrical machines based on electromagnetic field. The development of electroactive materials provides new promising opportunities to designed a new type of electromechanical actuators based on piezoelectric transducers. Generally, modern piezoelectric transducers are design using either quasi-static or resonant actuators. Modern piezoelectric motors are generally built using resonant structures.

An ultrasonic piezoelectric motor is an actuator that uses a mechanical vibration in the ultrasonic wave range as its driving source. The principle of operation of these actuators is based on the resonant mode activity of a mechanical structure, which is generating a kinematic interface transforming micro travel movements of large amplitude.

The piezoelectric motors are well known for their advantages like torque/mass ratio, quick start/stop response and holding torque. Due to their low efficiency, they are widely used only in low-power and low-duty cycle devices, especially in aerospace and space industry [4]-[8].

This paper presents the analytical model of the prototype piezoelectric multicell motor. The operation principle, design process and experimental results of this prototype motor have been presented in [1]. Also, the results of the analytical analysis were compared with FEM simulation and the measurement results.

In this paper the developed analytical model of the multicell piezoelectric motor is based on Timoshenko beam theory [9]. Also, the theoretical analysis of operating principle of the rotating mode motor has been described. Additionally the stator/rotor friction contact has been considered. Using the analytical model some electromechanical characteristics of the considered multicell piezoelectric motor have been computed. Finally, computed and measured characteristics have been compared.

II. OPERATING PRINCIPLE

Generally, the piezoelectric motors are made of four parts: stator, rotor, piezoelectric ceramics and power supply (Fig. 1). The stator made of piezoelectric material (ceramics) is associated with a mechanical structure (contre-mass). The piezoelectric ceramics are supplied and therefore deformed at a frequency corresponding to the mechanical resonance frequency of the structure. Thus, the initial deformation of ceramics is amplified by the effects of the resonance of the mechanical structure. The stator of a rotating-mode motor uses two modes of bending due to two electrical sources with 90° phase shifting (Fig. 1).

Two electrical sinusoidal sources are required to obtain the bending mode operation (Fig. 1). However, it is not enough to generate only the traveling wave. The specific orientation of the ceramics is necessary. The ceramics are situated between two contra-masses.

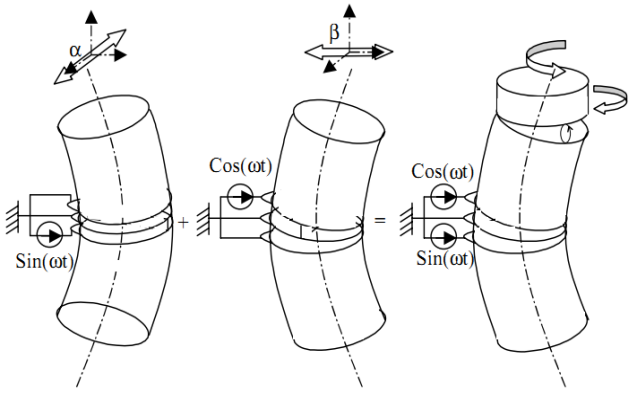

Fig. 1. Operation principle of a rotation mode motor [4]

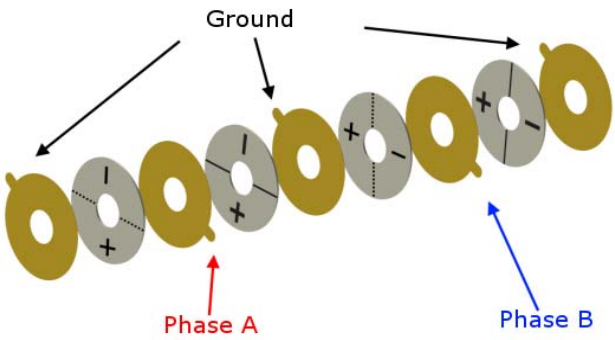

Fig. 2. Piezoelectric ceramics which are properly positioned

They have opposing polarization and are orthogonally at each other (Fig. 2). The traveling wave in the ends of the stator is developed, when each mode of bending is excited.

Finally, a special power supply source of high frequency voltage is needed (from few a to several kilo hertz)

A. Timoshenko beam theory

In literature the beam theory was well described by a Stephen Timoshenko [9]. The model takes into account shear deformation and rotational inertia effects, making it suitable for describing the behavior of short beams, sandwich composite beams or beams subject to high-frequency excitation, when the wavelength approaches the thickness of the beam. The basic motion equation is:

$$\mathrm{EI}\frac{\partial^4 u}{\partial z^4}+\rho A\frac{\partial^2 u}{\partial t^2}-\rho I(1+\frac{E}{aG})\cdot\frac{\partial^4 u}{\partial z^4\partial t^2}+ +\frac{\rho^2 I}{aG}\cdot\frac{\partial^4 u}{\partial t^4}=0 \quad (1)$$

And as results:

$$u(x)=A\sin(k_1 x)+B\cos(k_1 x)+ +C\sinh(k_2 x)+D\cosh(k_2 x) \quad (2)$$

It is possible to isolate the two quantities, like moment of inertia I, and a cross sections A . The additional quantities are: u – displacements, T – torque, F – share force, and Ψ – rotational angle.

B. Stator kinematics

Based on the literature [3]-[7], the traveling wave principle will be explained.

As it was said in first paragraph, to obtain a traveling wave two electrical sources with 90° phase difference are needed, and phases of the motor (piezoelectric ceramics) have also to be placed orthogonally at each other. Each of these phases generate the vibrations, which are perpendicular (Fig. 3). It can be assumed that stator has circular form.

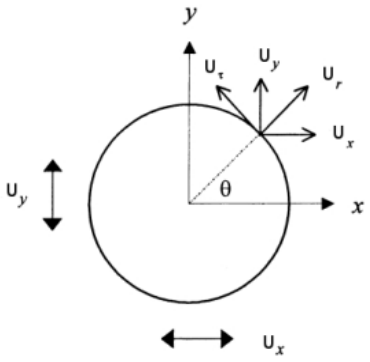

Fig. 3. Stator (contra-mass) deflections

The basics bending modes U_x and U_y in two axes are:

$$U_x=U_0\cos(\omega\cdot t) \quad (3)$$

$$U_y=U_0\sin(\omega\cdot t) \quad (4)$$

The superposition of two standing waves can generate traveling wave components. So, it is necessary to consider the deflections in circumferential and radial directions due to circular form of the stator - the values U and U_r are equal to:

$$U_\tau=U_x\cos\varphi+U_y\sin\varphi \quad (5)$$

$$U_r=U_y\cos\varphi-U_x\sin\varphi \quad (6)$$

And after transformation, using the (3), (4) and trigonometric identities:

$$U_\tau=U_0\cos(\omega\cdot t-\varphi) \quad (7)$$

$$U_r=U_0\sin(\omega\cdot t-\varphi) \quad (8)$$

The longitudinal displacements have to be considered also (Fig. 4). These displacements are generating from deflections (3) and (4), where r is a radius of the cross section.

Substituting the equations (3), (4) to the (9) and (10), the displacements might be expressed as follow:

$$u_x=-x\frac{\partial U_x}{\partial z}=-xU_0'\cos(\omega\cdot t) \quad (9)$$

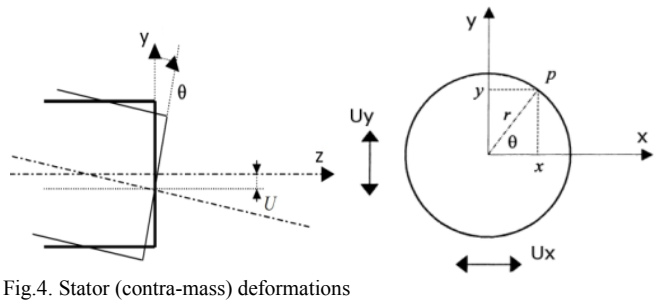

Fig.4. Stator (contra-mass) deformations

$$u_y = -y\frac{\partial U_y}{\partial z} = -yU_0^{'}\sin(\omega \cdot t) \qquad (10)$$

Finally, trigonometric identities from Fig. 4:

$$u_x = -r\cos\varphi \cdot U_0^{'}\cos(\omega \cdot t) \qquad (10)$$

$$u_y = -r\sin\varphi \cdot U_0^{'}\sin(\omega \cdot t) \qquad (11)$$

For the sum of the (11), (12), where u is a traveling wave:

$$\begin{aligned} u &= u_x + u_y \\ &= -r\cos\varphi \cdot U_0^{'}\cos(\omega \cdot t) - r\sin\varphi \cdot U_0^{'}\sin(\omega \cdot t) \\ &= -rU_0^{'}\cos\varphi(\omega \cdot t - \varphi) \end{aligned} \qquad (12)$$

Juxtaposition of the equitation's.

$$\left.\begin{aligned} U_\tau &= U_O\cos(\omega \cdot t - \varphi) \\ U_r &= U_O\sin(\omega \cdot t - \varphi) \\ u &= -rU_0^{'}\cos\varphi(\omega \cdot t - \varphi) \end{aligned}\right\} \qquad (13)$$

The traveling wave is made from two elliptical movements – tangential (u and U) and radial (u and U_r). Driving movements consist due to tangential movements. Final equitation for "useful" movements is:

$$\left(\frac{U_\tau}{U_0}\right)^2 + \left(\frac{u}{rU_0^{'}}\right)^2 = 1 \qquad (14)$$

The contact between stator and rotor take place where u reaches maximum value. Movement radial is movement parasite; it doesn't have much influence on tangential movement.

In this paragraph the theoretical analysis of the traveling wave has been described and generation of the displacements was shown.

C. Torque

In previous paragraph the tangential movements has been calculated. So now, it is possible to obtain the tangential velocity (Fig. 5). In this paragraph torque will be calculated also.

The tangential velocity is taken from (14):

$$V = U_\tau = U_0\omega\cos\left(\frac{x}{r}\right) \qquad (15)$$

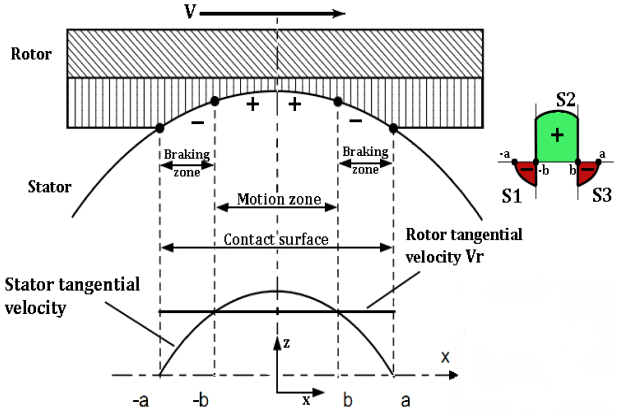

Fig. 5. Tangential velocity and friction distribution

Based on the Fig. 5 the surface between "*b*" points corresponds the rotor speed V_r. So, taking the equitation (16) and doing the transformation it is possible to calculate this coordination:

$$V = U_\tau = U_0\omega\cos\left(\frac{b}{r}\right) \longrightarrow b = R\cos^{-1}\left(\frac{V_r}{U_0\omega}\right) \qquad (16)$$

The rotor movement's directions depend on the negative or positive values. Negative when $V<V_r$ and positive $V>V_r$.

As explained, the rotation speed of the rotor corresponds to the integral of the speed of each point of the contact zone stator/rotor. It should be noticed that all the points of the driving area tend to pull the rotor for a speed greater than the relative speed of the rotor. Opposite, all points in the braking zone tend to slow down the relative velocity for a smaller than the rotor. Consider that there is a point "*b*" being identical to the rotor relative velocity (17). Assuming that the friction coefficient is constant, it can be concluded that contact surface is divided into three zones – S2 as a motions area, S1 and S3 as a braking zone. These surfaces represent the tangential friction, which is in fact the image of the torque.

The point "*d*" on the curve Fig. 6, correspond for rotor speed - when torque is null – the sum of the three surfaces is $S1+S2+S3=0$. So, there is a balance between the driving force and braking forces when the motor has no load.

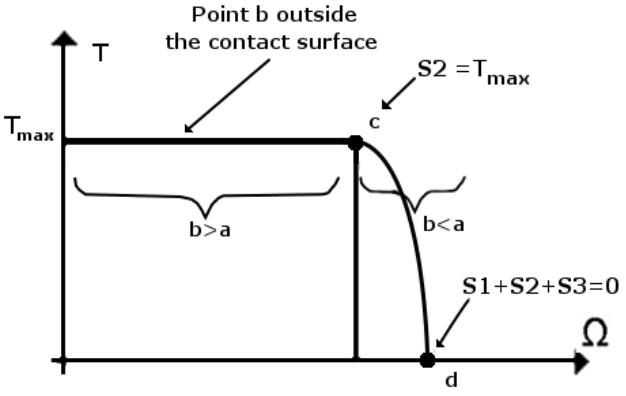

Fig. 6. Torque/speed curve

If load is changing, the motor speed will decrease, point "*b*" will move to the zone where the braking points are lower, until reach the surface of the contact area which was previously called "*a*". When *a=b* can be said that the torque is maximum, as the surface *S2* obtain the maximum value. If the motor load stays continuously, the point "*b*" will move outside the contact surface (but this has no affect for the torque), therefore the curve torque/speed is still linear.

The theoretical torque for *b<a* it can be calculated from:

$$T = 2\mu r \cdot \left(\int_0^b p(x)\omega dx - \int_b^a p(x)\omega dx \right) \qquad (17)$$

And for b>a, after transformation:

$$T_{\max} = \frac{\pi}{2}\mu \cdot a \cdot \omega \cdot r \cdot P_0 \qquad (18)$$

where: $p = P_0\left(1 - \left(\frac{x}{a}\right)^2\right)^{\frac{1}{2}}$ is pressure distribution, μ is friction coefficient, x is the position on the external perimeter of the stator.

III. MODELLING

The multicell piezoelectric motor is a combination of the traveling wave motor and piezoelectric rotating-mode motor. It combines the advantages of both motors, due to mixing of the three rotation mode actuators (Fig. 7).

The main goal of the project was to obtain a resonance frequency greater than 20 kHz (it is inaudible to the human ear).

Existing results of simulations and measurements of the multicell piezoelectric (Fig. 8) based on the design and simulation using FEM software. When the final shape of the stator (contra-masse) was performed the simulation in Autodesk Multiphysics has been done.

Fig. 7. Stator – contra-mass of the multicell piezoelectric motor

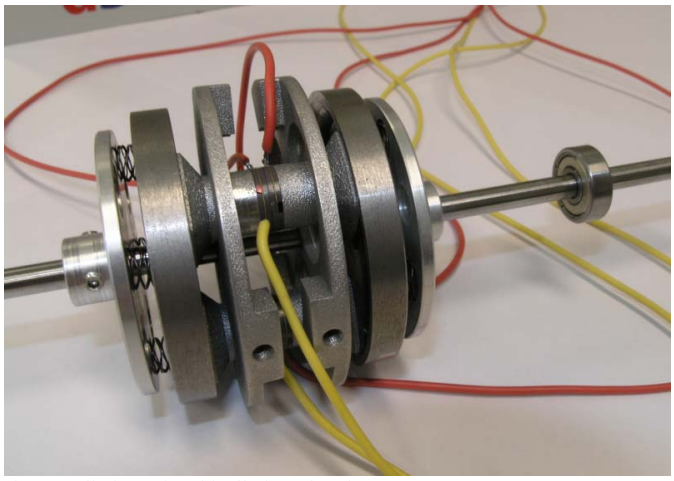

Fig. 8. Full view of multicell piezoelectric motor

The final simulation gave the resonance frequency about 25.6 kHz. After developing the prototype, the resonance frequency has been measured. The measurements were performed on the each phase (*A* and *B*) of the actuator. As a result of regulation and measurements, mechanical resonance was set to about 21.5 kHz.

Next step of the multicell piezoelectric motor analysis was analytical modelling to obtain the torque/speed curve. Based on the existing works in [4] and [5], where the design process of the cylindrical rotating-mode motor was described, model of the multicell piezoelectric motor was performed. Due to the complicated shape of the contra-mass some issues have been considered.

First, single actuator has two different dimensions on the endings. The cross-section of actuator doesn't have the regular shape. All these geometrical differences are clearly visible in Fig. 7.

Another issue was the contact between rotor and stator (in this case with three actuators) is not permanent and occurs only on three surfaces. Using this kind of solution, makes the structure more stable compared to regular rotating-mode motor because stator generate three traveling waves.

Finally, the torque of the motor should be considered due to one rotor and three resonance actuators.

IV. EXPERIMENTAL AND SIMULATION RESULTS

Analytical model of the multicell piezoelectric motor, taking into account dimension of the stator and piezoceramics ceramics, has been developed in Matlab environment. The materials used in simulation were: aluminum in contra-mass, PZT 89 in ceramics and steel for the rotor.

The results are presented in Fig. 9- Fig.11. The differences between Multiphysics FEM method and analytical simulation are not big, the values are satisfying. Compared with measurements obtained by impedance analyzer where resonance respond was in 21.5 kHz, the difference is around 4 kHz. The contremases are not twisted enough which are causing lower resonance frequency. Problems are with proper orientation of the piezoceramics appeared also.

The maximum torque was calculated from approximation of the torque obtained in single actuator. The result is about 0.6 Nm. It should be noticed that is a theoretical curve because some coefficients are constant (exp. friction coefficient). The maximal torque is changing due to the applied force from the rotor. In the experimental results rotational velocity was around 48 rpm and blocking torque 0.4 Nm (fig. 11).

The overall mechanical losses of the motor are the sum of losses in the vibrating stator and losses due to the contact.

The stator's mechanical dissipation losses are comparable to the power generated at the contact amplitudes. Reduction of these mechanical losses would increase the rotational speed or torque of the motor for the same power supply voltage.

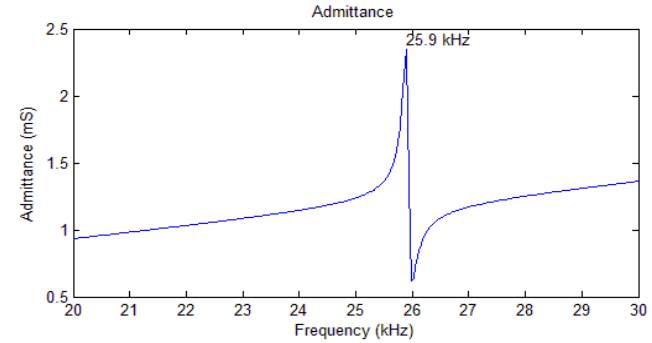

Fig. 9. Simulations of the resonance frequency results

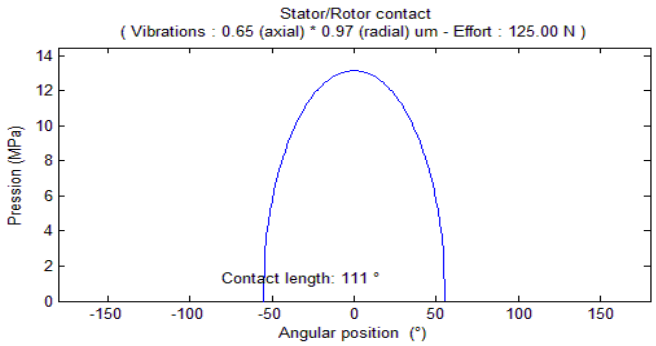

Fig. 10. Stator/Rotor contact pressure

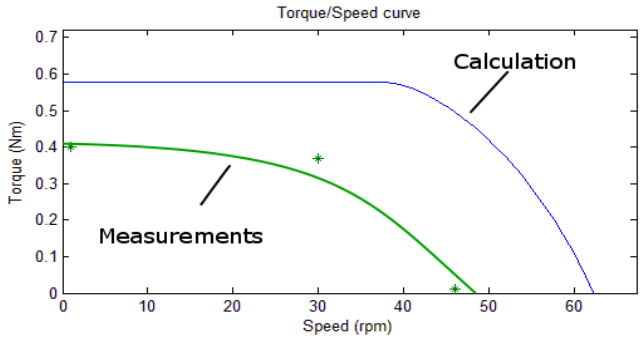

Fig. 11. Torque/speed curve

Finally, to obtain the overall model behavior of the motor, it is necessary to take into account the stator/rotor contact surface. In simulation the radial displacements have 0.97 µm and supply voltage around 400 V. Prototype displacements measurements gave 0.55 µm with 100 V power supply. Due to the value does not increase linearly; it can be assumed that the result is correct.

V. CONCLUSION

This paper presents analytical model of the multicell piezoelectric motor. The results, obtained in the field of piezoelectric motors, have pointed out that these motors have potentially high possibilities in future special applications. The studied multicell piezoelectric motor have a stator using three rotating mode actuators. A theoretical analysis of operating principle of the rotating mode motor has been described. Additionally the stator/rotor friction contact has been considered. Using the analytical model some electromechanical characteristics of the considered multicell piezoelectric motor have been computed. Finally, computed and measured characteristics have been compared.

REFERENCES

[1] R. Ryndzionek, J-F. Rouchon, M. Ronkowski, M. Michna, and L. Sienkiewicz, Design, "Modelling and analysis of a new type of piezoelectric motor. Multicell piezoelectric motor", *IECON 2013 - 39th Annual Conference of the IEEE*, pp. 3910-3915, Nov. 2013

[2] T. Sashida, T. Kenjo, "An introduction to ultrasonic motors", *Oxford, Clarendon Press*, 1993

[3] P. Lua, K.H. Lee, S.P. Limb and W.Z. Lin, "A kinematic analysis of cylindrical ultrasonic micromotors", *Sensors and Actuators*, A 87, pp. 194-197, 2001

[4] M. Budinger, J-F. Rouchon and B. Nogarede, "Analytical modeling for the design of a piezoelectric rotating-mode motor", *IEEE Trans. On Mechatronics,* vol. 9, NO.1, March 2004

[5] M. Budinger, J.-F. Rouchon, B. Nogarede, "A mason type analysis of cylindrical ultrasonic micromotors", *European Physical Journal Applied Physics 25*, pp. 57-65, 2004.

[6] B. Nogarede, "Moteurs piezoelectriques", *Techniques de L'ingenieur,* L'expertise technique et scientifique de référence, 1996

[7] N.W. Hagood IV and A.J. McFarland, "Modeling of a Piezoelectric Rotary Ultrasonic Motor", *IEEE Trans. On Ultrasonics, Ferroelectrics, And Frequency Control*, vol. 42, No. 2, pp. 210-224, March 1995

[8] A. Iula and M. Pappalardo, "A High-Power Traveling Wave Ultrasonic Motor", *IEEE Trans. On Ultrasonics, Ferroelectrics, And Frequency Control*, Vol. 53, No. 7, pp. 1334-1351, July 2006

[9] W. Weaver Jr., S.P. Timoshenko, D.H. Young, "Vibration Problems in Engineering", 5th Edition, Wiley, New York, 1990

[10] W. Szlabowicz, J-F., Rouchon, B. Nogarede, "Design and realization of a rotating-mode piezoelectric motor for aeronautic applications", *10th International Conference on New Actuators*, 14-16 June, Bremen, Germany, 2006.